

Adsorption of Lead, Manganese, and Copper onto biochar in landfill leachate: implication of non-linear regression analysis

Ali Daryabeigi Zand (✉ adzand@ut.ac.ir)

University of Tehran

Maryam Rabiee Abyaneh

University of Tehran

Research

Keywords: Adsorption, biochar, landfill leachate, heavy metals, linearization error

Posted Date: August 22nd, 2020

DOI: <https://doi.org/10.21203/rs.3.rs-26558/v3>

License:  This work is licensed under a Creative Commons Attribution 4.0 International License.

[Read Full License](#)

Version of Record: A version of this preprint was published on September 9th, 2020. See the published version at <https://doi.org/10.1186/s42834-020-00061-9>.

1 **Adsorption of Lead, Manganese, and Copper onto biochar in landfill leachate:**
2 **implication of non-linear regression analysis**

3 **Ali Daryabeigi Zand* and Maryam Rabiee Abyaneh**

4 School of Environment, College of Engineering, University of Tehran, Tehran 141556135, Iran

5

6

7

8

9

10

11

12

13

14

15 * Correspondence: adzand@ut.ac.ir

16 **Abstract**

17 The feasibility of using wood-derived biochar (BC) to remove Pb, Mn, and Cu from landfill
18 leachate was investigated and modeled in this study. BC was produced under the pyrolytic
19 temperature of 740 °C. The effect of contact time, BC dosage and particle size on adsorption of
20 the heavy metals onto BC was examined. BC was used in two forms i.e., pulverized (PWB) and
21 crushed (CWB) to evaluate the effect of BC particle size on adsorption characteristics. The
22 kinetics of Pb, Mn, and Cu adsorption onto PWB and CWB were assessed using the pseudo
23 second-order and Elovich models, where both applied models could well describe the adsorption
24 kinetics. Removal efficiencies of the heavy metals were increases by 1.2, 1.4, and 1.6 times,
25 respectively, for Pb, Mn, and Cu, when PWB content of the leachate increased from 0.5 to 5 g L⁻¹. Equilibrium adsorption capacity of the heavy metals onto BC in leachate system was evaluated
26 using the Langmuir, non-linearized Freundlich, linearized Freundlich, and Temkin isotherms and
27 found to have the following order for PWB: Non-linearized Freundlich > Temkin > Langmuir >
28 Linearized Freundlich. The Langmuir and linearized Freundlich models could not adequately
29 represent adsorption of the heavy metals onto BC, especially for CWB. The highest removal of
30 88% was obtained for Pb, while the greatest adsorption intensity was found to be 1.58 mg g⁻¹ for
31 Mn. Using the non-linearized Freundlich isotherm significantly reduced adsorption prediction
32 error. The adsorption affinity of PWB for Pb, Mn, and Cu was greater than that of CWB in all
33 treatments. Wood-derived BC is suggested to be used for the removal of heavy metals from
34 landfill leachate as an economical adsorbent.

36

37 **Keywords:** Adsorption, biochar, landfill leachate, heavy metals, linearization error

38

39 **1. Introduction**

40 Landfill leachate may contain a wide range of contaminants at levels enough to raise serious
41 environmental and human health concerns. The majority of published research has focused on
42 removal of ammonia and organic fraction of landfill leachates, such as using biological reactors
43 [1], oxidation processes [2] and membrane separation [3]. Concentrations of heavy metals in
44 fresh landfill leachate, characterized by lower pH, are usually higher than those in aged leachate
45 [4]. Adsorption of heavy metals on carbonaceous materials has received considerable attention to
46 remove toxic metals from contaminated aqueous solutions. Salam investigated the removal of
47 heavy metals from synthetic aqueous solution by adsorption onto carbon nanotubes through a set
48 of batch experiments which showed effective removal of heavy metals [5]. Activated carbon
49 (AC) is a well-known strong adsorbent which has been employed to remove heavy metals from
50 different media principally because of its large surface area and high porosity [6-8]. Palm shell
51 AC was successfully used to remove Cu from aqueous solution [9]; but high production expenses
52 of AC may limit its use as adsorbent [10]. Application of economical alternatives to AC has
53 therefore drawn remarkable attention in recent years. For instance, in a study by Soco and
54 Kalembkiewicz, coal fly ash was successfully used for the removal of nickel and copper from a
55 synthetically contaminated aqueous solution [11].

56 Adsorption process rate is usually studied using kinetic models, while the variation in the
57 amount of sorbate adsorbed by different doses of adsorbent is evaluated by isotherm models,
58 which is critical in optimizing the use of adsorbents. Various models have been proposed to
59 study adsorption of heavy metals onto carbonous materials in aqueous solutions [12-14]. The
60 adsorption kinetics of Pb and Zn onto carbon nanotubes in aqueous solutions were described well
61 using pseudo-second-order and Elovich models. Lagergren pseudo-first-order model was not

able to predict adsorption kinetics of the metals as precise as pseudo-second-order and Elovich models [5]. The applicability of the pseudo-second-order and Elovich models to predict adsorption kinetics of heavy metals in contaminated aqueous solutions has been reported in the literature [15-17]. Temkin isotherm model assumes that the heat of adsorption of all the molecules in layer declines as adsorbent surface coverage increases due to adsorbate-adsorbate repulsions. Fall in the heat of adsorption is considered to be linear for Temkin isotherm rather than logarithmic. Adsorption of adsorbate onto adsorbent is also characterized by a unisonous distribution of binding energies up to ca. maximum binding energy [14]. Adsorption of chlorophenoxyacetic acid herbicides from water onto orange peel AC was successfully described by Temkin isotherm model [18]. Moreover, the Temkin model could satisfactorily predict adsorption of Cr(VI) onto AC, though higher R^2 values were found using the Freundlich and Langmuir equations [19]. Freundlich and Langmuir equations are the most well-known models for describing adsorption isotherm [20]; but applying non-linearized form of the Freundlich model in adsorption studies has been scant. Isotherm and kinetic models are often applied in linear form, though linearization of the original model might violate the theories and assumptions behind the development of a given model. That means when model parameters are estimated based on linear transformation it would not necessarily yield the best fitting parameters for the nonlinear original model [21]. Error analysis for the kinetic and isotherm models, which has rarely been studied in adsorption of heavy metals onto biochar (BC) in landfill leachate, was also investigated in this paper.

Recently, use of BC has attracted considerable attention [22]. de Caprariis et al. employed BC to remove total organic carbon from wastewater, and a very high sorption capacity of BC (840 mg g^{-1}) was achieved [23]. In another study, BC derived from sewage sludge eliminated Cr

85 from water significantly by 89%, whereas As removal did not exceed 53% [24]. Many studies
86 have focused on the immobilization and mitigation of contaminants, respectively, in soil and
87 effluents [25, 26]; however, removal of heavy metals from landfill leachate by BC has rarely
88 been investigated. This research aimed to investigate the adsorption of Pb, Mn and Cu onto
89 wood-derived BC in fresh landfill leachate. We specifically studied: (i) effect of contact time,
90 BC dosage and particle size on adsorption of heavy metals onto BC; (ii) adsorption kinetics of
91 the heavy metals onto BC in landfill leachate using pseudo second-order and Elovich models;
92 and (iii) modeling of adsorption of the heavy metals onto BC in landfill leachate using
93 Freundlich (linearized and non-linearized), Langmuir and Temkin isotherms.

94

95 **2. Materials and methods**

96 *2.1. Site description and leachate sampling and analysis*

97 Kahrizak landfill which is also known as Aradkooh waste disposal and processing complex
98 is main disposal site of the capital city of Tehran, located at a 25 km distance from the southern
99 part of the capital city of Tehran having longitude of $51^{\circ}19'18''$ E and latitude of $35^{\circ}27'52''$ N.
100 More than 8 kt of wastes are transferred daily to the landfill site. Household hazardous wastes
101 are buried together with general wastes. Generated leachate at Kahrizak landfill is a serious
102 environmental and health threat. High clay content and therefore low permeability of the land
103 around the landfill caused infiltration of the landfill leachate to be minimal. Therefore, freshly
104 generated leachate at Kahrizak landfill, which is now estimated to be about $637 \text{ m}^3 \text{ d}^{-1}$ [27],
105 flows gravitationally towards the low land next to the burial site creating a leachate lake with a
106 depth of ca. 10 m, with seasonal variations. In this study, the leachate samples were directly
107 collected from the generated leachate stream at the bottom of the waste discharge place at

108 Kahrizak landfill and used for the adsorption experiments. Overflow of the fresh leachate from
109 newly-filled trenches was directly collected in four 10-L plastic containers. Collected leachate
110 can be classified as relatively fresh leachate based on the low pH values (5.11). Leachate
111 samples were immediately transported to the laboratory. Samples were kept refrigerated at 4 °C
112 without exposure to the ambient air for not more than three days before conducting relevant
113 analysis to prevent potential chemical and biological changes.

114 Leachate samples characterized according to the Standard Methods for the Examination of
115 Water and Wastewater [28]. Raw samples were filtered using Whatman Paper Filter No. 1 (pore
116 size: 11 µm) prior to acid digestion in order to remove particles larger than 11 µm. Leachate
117 samples were digested with nitric acid, then the digestate passed through MILEXHA 0.45 µm
118 diameter filter followed by the US EPA 3005A method [29]. Partially filtered samples containing
119 suspended particles (up to 11 µm) were analyzed for heavy metal content to imitate close to real
120 conditions, as when landfill leachate is analyzed to control compliance with permissible limits.
121 Samples were digested in triplicate and analyzed for the concentrations of Cd in the final
122 solution using an atomic absorption spectrometer (Perkin Elmer 700). Organic load of the
123 leachate produced at this landfill is markedly higher than that of leachate generated in many
124 other countries [13, 30]; due to the high content of organics such as food wastes. Received
125 municipal solid wastes at Kahrizak landfill is characterized by putrifiable fraction of ca. 68% and
126 moisture content of 65-70% that significantly contribute to high organic load of produced
127 leachate. Elevated ratio of biological oxygen demand (BOD)/chemical oxygen demand (COD)
128 for landfill leachate as observed in this study indicates the high concentration of biodegradable
129 organic compounds in leachate, and hence a good potential to be biologically degraded. Some
130 characteristics of the leachate are as follow: COD (71245 mg L⁻¹); BOD (32187 mg L⁻¹);

131 BOD/COD (0.45); Total suspended solids (19800 mg L⁻¹); Total dissolved solids (11480 mg L⁻¹); NO₃-N (70 mg L⁻¹), SO₄ (1698 mg L⁻¹); electrical conductivity (28.86 mS cm⁻¹); pH (5.11)
132 and Pb (1.90 mg L⁻¹), Mn (7.78 mg L⁻¹) and Cu (2.52 mg L⁻¹) [28].
133

134 *2.2. BC preparation*

135 Fresh urban yard trimmings with no pollution background was initially chopped into wood
136 chips of 5-10 cm length and then oven-dried for 48 h. Yard trimmings can be found abundantly
137 in most places and often used for composting or find their way into urban waste stream. Dried
138 wood chips were placed in open crucibles, then weighted, and covered thoroughly with
139 aluminum foil in order to provide an oxygen-limited environment. BC derived from the wood
140 chips was produced under the pyrolytic temperature of up to 740 °C with a temperature gradient
141 of ca. 10 °C min⁻¹ until the desired temperature of 740 ± 5 °C was reached in the muffle furnace
142 under the atmospheric pressure with residence time of 42 min. At the end, samples were kept in
143 the furnace overnight to let them cool down to the room temperature. The produced BC chips
144 were air-dried over a week, ground using a ceramic mortar and pestle and sieved to gain
145 homogenous crushed wood-derived BC (CWB), with the particle size of 1 to 2 mm. Moreover,
146 some BC chips were further ground and sieved to 63-75 µm diameter to yield fine-graded BC to
147 be used as pulverized wood-derived BC (PWB) in the adsorption experiments. Elemental
148 composition of the produced BC was as follow (dry basis): C (81.5%), O (11.2%), H (3.3%), N
149 (0.5%), S (0.1%) and ash (3.4%). The produced BC had particle density of 1.5 g cm⁻³. PWB and
150 CWB had bulk densities of 0.93 and 0.69 g cm⁻³, respectively. The pH of the BC (9.1) was
151 determined following the method of Singh et al. [31]. BET surface area was measured using a
152 Brunauer-Emmett-Teller Surface Area & Porosity Analyzer (NOVA 4200e) by nitrogen gas
153 sorption analysis at 77 K. Samples were vacuum degassed prior to analysis, at 300 °C for 5 to 15

154 h, based on the required time to reach a stable surface area measurement [32]. BET surface area
155 of the PWB and CWB were determined to be 335 and 281 m² g⁻¹, respectively.

156 *2.3. Adsorption experiment*

157 The adsorption process of Pb, Mn and Cu was conducted under the adjusted pH of 5.1 in
158 order to eliminate the possibility of formation of metal hydroxide precipitates. Solutions were
159 initially adjusted for the desired pH, and then the BC was added. Values of pH were measured
160 during the experiments once (for experiments below 600 min) or twice (for experiments longer
161 than 600 min) for probable pH adjustment. Precipitation of heavy metal hydroxides between the
162 pH values of 6.5-7 was reported for heavy metals [33]. Adsorption of heavy metals onto PWB
163 and CWB was carried out versus time at specified intervals up to 24 h. Actual concentrations of
164 Pb, Mn and Cu ions in leachate samples were considered as the initial concentration, to simulate
165 real conditions. Each adsorption experiment was conducted in triplicate and the mean values
166 were reported. The percentage removal of heavy metals in the solution was calculated using the
167 following equation

$$168 R(\%) = \frac{C_0 - C_e}{C_0} \times 100 \quad (1)$$

169 Where, C₀ and C_e are, respectively, the initial and final concentrations of Pb, Mn and Cu in
170 leachate samples (mg L⁻¹). Kinetic solutions were stirred on a shaker at constant rate of 120 rpm
171 at room temperature of 24 ± 2°C to provide effective interaction of sorbate with sorbent material.
172 At the end of the specified agitation period, obtained mixtures were centrifuged for 15 min at
173 6000 rpm to separate liquid and solid phases, filtered by Whatman Paper Filter No. 1 (11 µm
174 pore size) and the filtrates were then analyzed for the heavy metal concentrations. The adsorption
175 isotherms were studied in actual leachate system for Pb, Mn and Cu. Certain quantities of PWB
176 and CWB (0.05 to 5 g) were separately weighted and added to a 100 mL fresh landfill leachate at

177 initial pH of 5.1. The pseudo first-order, pseudo second-order and Elovich models were used to
178 study the kinetics of adsorption of Pb, Mn and Cu onto BC in landfill leachate and the Langmuir,
179 non-linearized and linearized Freundlich, and Temkin isotherm models were applied to fit the
180 measured data.

181 *2.4. Error analysis for the kinetic and isotherm models*

182 Non-linear regression as a more general technique to estimate parameters of adsorption
183 models can be used even if the model cannot be linearized. However, isotherm and kinetic
184 models are mainly applied in linear form because less difficult calculations are required to find
185 model parameters. It should be noticed that modifying and linearization of the original model
186 might violate the theories and assumptions behind the development of a given model that means
187 when parameters are estimated based on linear transformation of a given model it does not
188 necessarily yield best fitting parameters for the nonlinear original model [34]. Error structure of
189 experimental data has been found to be altered when adsorption isotherms transformed into
190 linearized forms. Non-linear regression usually minimizes the error distribution between the
191 experimental and predicted data, unlike linear regression [35]. Therefore, linear determination
192 coefficient (R^2) should be used to measure the matching degree between experimental and
193 predicted data when linear form of a given adsorption kinetic or isotherm model is applied.
194 Beside linear R^2 , the applicability of the applied models can also be verified through error
195 analysis techniques such as sum of error squares (SSE). The SSE is said to be among the
196 widespread used error functions. It can be written as:

197

198
$$SSE(\%) = \frac{\sqrt{\sum (q_{e(Exp)} - q_{e(Cal)})^2}}{N} \quad (2)$$

199 Where, $q_{e(\text{Exp})}$ is the adsorption capacity at equilibrium condition obtained from adsorption
200 experiments, $q_{e(\text{Cal})}$ is the calculated value of adsorption capacity at equilibrium state, and N is
201 the number of data points [36].

202 **3. Results and discussion**

203 *3.1. Effect of contact time on the adsorption of Pb, Mn, and Cu onto BC in the leachate*

204 The effect of contact time on the adsorption of Pb, Mn, and Cu in landfill leachate is shown
205 in Fig. 1a and 1b. The adsorbent dosage was fixed at 1 g 100 mL⁻¹ (10 g L⁻¹) and the pH value of
206 the fresh leachate was 5.1. The removal efficiency of the heavy metals experienced a drastic
207 initial increase followed by a gradual rise to reach a plateau, which indicates equilibrium
208 condition. Instant adsorption rate of heavy metals onto BC gradually declined to zero with the
209 equilibrium point of adsorption lay between 150-200 and 100-150 min for, respectively, PWB
210 and CWB, suggesting that the contact time of 200 and 150 min is sufficient to establish dynamic
211 balance. The importance of contact time to provide sufficient contact between adsorbates and
212 adsorbent surface has been emphasized by several authors [35, 37]. It can be inferred from Fig.
213 1a and 1b that the removal of Pb, Mn, and Cu was greater when PWB was used as adsorbent,
214 compared to CWB. Moreover, longer period of contact time was required for the equilibrium
215 state to be established when BC with smaller particle size, i.e., PWB was used, implying slower
216 occupation of adsorption sites on the surface of PWB due to the greater specific surface provided
217 by PWB relative to CWB. The highest removal efficiency of 88% by PWB was obtained for Pb.

218 As reaction time prolonged, repulsive forces between the metal ions adsorbed to BC and
219 those in the aqueous phase might be increased. In addition, unoccupied adsorption sites and
220 therefore adsorption efficiency will be quickly declined until the establishment of dynamic
221 balance in the system. The same observation was found for Ni uptake from aqueous solution by

222 AC derived from sugar bagasse [37]. From the adsorption diffusion viewpoint, two distinct
223 adsorption stages could be distinguished for the uptake of Pb, Mn, and Cu onto BC in landfill
224 leachate; surface diffusion during which the mass transfer is rapid and physical processes control
225 the adsorption, followed by intra-particle diffusion that is characterized by slow adsorption.
226 Greater adsorption efficiency for heavy metals was observed for all the applied dosages of BC at
227 initial stages of the experiment, that may be attributed to the higher availability of adsorption
228 sites on BC surface which are rapidly occupied by the solutes in the leachate. When equilibrium
229 is reached mass transfer from the leachate to the surface of BC was significantly restricted (Fig.
230 1a and 1b), which is consistent with those reported in the literature [13].

231

232 *3.2. Effect of BC dosage on the adsorption of heavy metals in landfill leachate*

233 BC dosage varied from 0.05 to 5 g 100 mL⁻¹ (0.5 to 50 g L⁻¹) at initial pH of 5.1, with the
234 reaction times of 200 and 150 min, respectively, for PWB and CWB. Results indicated that the
235 removal efficiency of the heavy metals was significantly raised by 1.2, 1.4, and 1.6 times,
236 respectively, for Pb, Mn, and Cu, when PWB content of the leachate increased from 0.5 to 5 g L⁻
237 ¹. Obtained results are consistent with the literature, where removal of Ni from aqueous phase
238 increased by AC dosage [37]. The removal efficiency of Pb, Mn, and Cu did not change
239 significantly as BC content exceeded 2 g 100 mL⁻¹ in leachate. It suggests the optimal dosage of
240 20 g L⁻¹ for both PWB and CWB to achieve the highest economical adsorption capacity for the
241 heavy metals. Unsaturated adsorption sites may increase as BC dosage exceeds the optimum
242 amount. The highest removal efficiency was obtained for Pb followed by Mn and Cu due to
243 addition of PWB (Fig. 1c) and CWB (Fig. 1d).

244 Removal efficiency of Mn and Cu was comparable, with slightly higher elimination for Mn.
245 Amount of Pb, Mn, and Cu adsorbed to each gram of BC reduced with rising adsorbent dosage,
246 likely due to the availability of more adsorption sites on the surface of both PWB and CWB.
247 Optimum AC dosage of 7 g 100 mL⁻¹ was found to effectively adsorb COD and NH₃ from
248 landfill leachate [13], which is markedly higher than the optimum dosage of BC obtained in this
249 study. It might be attributed to the higher levels of COD and NH₃ in leachate compared to those
250 of heavy metals in this study. BC dosage may also induce pH variation, which in turn affects
251 adsorption of adsorbates in aqueous systems by changing the adsorbent surface charge and
252 degree of ionization of adsorbates. Addition of high levels of BC to fresh leachate may increase
253 pH and promote the formation of metal hydroxides. However, adverse effect of low pH on
254 adsorption of Ni onto AC has been reported due to competence with hydrogen ions [38]. The
255 influence of pH on adsorption of heavy metals on various adsorbents has been well documented
256 [14].

257 *3.3. Adsorption kinetics*

258 Batch kinetic experiments were carried out for the adsorption of Pb, Mn, and Cu onto PWB
259 and CWB in landfill leachate. Lagergren pseudo-first-order model is also one of the most widely
260 used equations to describe adsorption kinetics. However, pseudo-first-order model was not able
261 to well describe adsorption kinetics of heavy metals onto carbonous materials in some studies
262 [5]. In addition, preliminary calculations conducted in this research indicated non-sufficient
263 description of adsorption kinetics of Pb, Mn and Cu onto PWB and CWB in the landfill leachate
264 (data not shown). Therefore, the kinetics for adsorption of heavy metals onto BC was simulated
265 using two kinetic models: pseudo second-order and Elovich kinetic models. The experimental
266 effectiveness is controlled by the adsorption kinetics. Adsorption kinetic models are typically

267 used to investigate the adsorption mechanism and the potential rate of the processes such as mass
268 transfer and chemical reactions [13].

269 *3.3.1. Pseudo second-order kinetic model*

270 The non-linear form of pseudo second-order model is represented as follow:

271
$$q_t = \frac{k_{2p} q_e^2 t}{1 + k_{2p} q_e t} \quad (3)$$

272 Where k_{2p} is the second-order adsorption constant ($\text{g mg}^{-1} \text{min}^{-1}$), q_e is the amount of heavy
273 metals adsorbed onto BC when dynamic balance researched (mg g^{-1}), and q_t is the amount of
274 adsorbate adsorbed onto BC at any time, t . In order to gain the linear form of the pseudo second-
275 order kinetic model the following equation should be solved through integration:

276
$$\frac{dq_t}{dt} = k_{2p} (q_e - q_t)^2 \quad (4)$$

277 If the boundary conditions of $q_t = 0$ to $q_t = q_t$ and $t = 0$ to $t = t$ is applied, the model can be
278 written as follows:

279
$$\frac{t}{q_t} = \frac{1}{k_{2p} q_e^2} + \frac{1}{q_e} t \quad (5)$$

280 Plots of t/q_t versus t for adsorption of Pb onto PWB and CWB are illustrated in Fig. 2.
281 Similar graphs could be constructed using the obtained data for Mn and Cu, with the same trend
282 as Pb. Figure 2a and 2b clearly illustrates higher adsorption capacity of PWB compared to CWB
283 for the heavy metals. The pseudo second-order kinetic constants and the theoretical q_e values
284 using the pseudo second-order expression are given in Table 1 for all the studied metals. Very
285 high values of R^2 (≥ 0.999) were found for the pseudo second-order kinetic model in all applied
286 levels of PWB and CWB indicating an excellent linearity. Results showed an excellent
287 agreement between the experimental data and the calculated adsorption capacity by the pseudo

288 second-order kinetic model which is consistent with the literature, where heavy metals in an
289 aqueous solution were removed by carbon nanotubes [5]. Error analysis indicated that deviation
290 occurred by application of the pseudo second-order kinetic model is very small for all levels of
291 BC, regardless of the BC particle size. This supports the chemisorptions theory behind the
292 pseudo second-order kinetic model for the heavy metals/BC system; however, evaluation of
293 variation of adsorption energy using appropriate isotherms such as Temkin model could provide
294 deeper insight into the nature of metal adsorption onto BC. It can be inferred from Table 1 that
295 the adsorption equilibrium rate for the studied heavy metals, regardless of the BC size, has the
296 following order: Pb > Cu > Mn. The applicability of pseudo second-order model to fit the
297 experimental kinetics data was also reported for adsorption of heavy metals onto sewage sludge
298 [24]. Predicted adsorption capacity decreased by increasing dosage of PWB and CWB. The
299 adsorption process is mainly a surface phenomenon and increase in adsorption sites on the
300 surface of an adsorbent at a constant adsorbate level could result in alleviated adsorption
301 intensity.

302 *3.3.2. Elovich kinetic model*

303 The Elovich adsorption kinetic equation which was initially developed to describe
304 chemisorption kinetics of gas onto solids [39], has recently gained increasing attention to
305 describe kinetics of adsorption of adsorbates in aqueous phase onto adsorbents. The Elovich
306 kinetic model is expressed as follows:

$$307 \frac{dq_t}{dt} = \alpha \exp(-\beta q_t) \quad (6)$$

308 Where α is the initial adsorption rate ($\text{mg g}^{-1} \text{ min}^{-1}$) and β is defined as desorption constant
309 (g mg^{-1}) during any experiment [36]. Elovich differential equation can be solved assuming $\alpha \beta_t$

310 >> 1 and by applying the boundary conditions of $q_t = 0$ at $t = 0$ and $q_t = q_t$ at $t = t$ [39]. Therefore,
311 the linear form of the Elovich equation can be presented as follows:

312
$$q_t = \frac{1}{\beta} \ln(\alpha \beta) + \frac{1}{\beta} \ln t \quad (7)$$

313 In order to study the adsorption kinetics using Elovich model a straight line of q_t versus $\ln t$
314 should be plotted to be able to calculate the model constants of α and β from the slope and the
315 intercept of the plot. For instance, Pb adsorption capacity of BC predicted by the Elovich kinetic
316 model is shown in Fig. 3. Parameters of the Elovich kinetic model for adsorption of Pb, Mn and
317 Cu onto PWB and CWB are presented in Table 2. Pretty high R^2 and low SSE values obtained
318 for the Elovich kinetic model suggesting that adsorption kinetics of the heavy metals onto BC in
319 landfill leachate can be adequately represented by the Elovich kinetic model. However, higher
320 values of R^2 and lower values of SSE were found for the pseudo second-order kinetic model
321 compared to the Elovich kinetic expression in this study. Comparison of the kinetic data obtained
322 in this study suggests pseudo second-order kinetic expression is the optimum kinetic expression
323 to represent adsorption of Pb, Mn, and Cu onto BC in landfill leachate.

324 *3.4. Modeling of adsorption isotherms*

325 The equilibrium data were modeled using the Langmuir, non-linearized Freundlich,
326 linearized Freundlich and Temkin isotherms in this study to predict adsorption capacity of PWB
327 and CWB for heavy metals in landfill leachate. Experimental data versus the predicted
328 adsorption of Pb, Mn and Cu onto BC in the leachate using different adsorption isotherms are
329 shown in Fig. 4. Experimental results indicated that Pb could be adsorbed on BC to a higher
330 degree than Mn and Cu. Adsorption of Mn on BC was comparable with that of Cu with slightly
331 higher adsorption for Mn.

332 *3.4.1. Langmuir isotherm*

333 The Langmuir model which is an empirical isotherm assumes uniform energies of
334 adsorption onto the adsorbent surface with no interaction between adsorbate molecules on
335 adjacent sites. All adsorption is also assumed to occur through the same mechanism to form a
336 layer with a thickness of one molecule on solid surface [25]. Once a site is occupied, no further
337 adsorption can proceed at that site based on the Langmuir isotherm representing the surface
338 saturation condition. Langmuir isotherm has been extensively used to evaluate adsorption
339 capacity of a wide range of contaminants such as heavy metals, organic pollutants and dyes [12].
340 Langmuir model describes a homogeneous adsorption assuming that all the adsorption sites on
341 the surface of a given adsorbent have equal solute affinity. It is also assumed that adsorption of
342 solute at one site does not affect the adsorption at an adjacent site [40]. Therefore, the maximum
343 adsorption capacity obtained by using the Langmuir isotherm is based on complete monolayer
344 coverage of the surface of adsorbent. All adsorption is assumed to occur through the same
345 mechanism. The non-linear expression of Langmuir isotherm model can be illustrated as follows:

$$346 \quad q_e = \frac{q_m b C_e}{1 + b C_e} \quad (8)$$

347 where, b is adsorption equilibrium constant (L mg^{-1}) which is related to the apparent energy
348 of adsorption, and q_m is the quantity of adsorbate required to form a single monolayer on unit
349 mass of a given adsorbent (mg g^{-1}).

350 Values of the constants for different types of linearized Langmuir isotherm are presented in
351 Table 3 for the adsorption of Pb, Mn and Cu onto BC. The applied linearized forms of Langmuir
352 isotherm equation is among the most frequently used linearized forms in the literature [41].
353 Langmuir isotherm can be further analyzed and the favorable nature of adsorption of adsorbate
354 onto adsorbent can be expressed through determination of the separation factor, R_L , which is a
355 dimensionless equilibrium parameter defined by the following equation:

$$356 \quad R_L = \frac{1}{1+bC_0} \quad (9)$$

357 Where b is the Langmuir model constant related to the free energy of adsorption ($L \text{ mg}^{-1}$).
 358 The R_L indicates the shape of the isotherm. Values of $0 < R_L < 1$ indicates favorable adsorption,
 359 whereas $R_L > 1$ represents an unfavorable adsorption. In addition, $R_L = 0$ represents irreversible
 360 adsorption, while the adsorption is linear if $R_L = 1$ [21, 42]. The dimensionless R_L values
 361 calculated for adsorption of the heavy metals onto PWB were between zero to one showing
 362 favorable adsorption, while the corresponding values for CWB were greater than 1 indicating an
 363 unfavorable adsorption (Table 3).

The values of R^2 and R_L obtained from Langmuir expression indicate positive evidence that the adsorption of Pb, Mn, and Cu onto PWB follows the Langmuir isotherm. The fit of the measured data to the Langmuir model reveals the possibility of sorption of the heavy metals onto PWB through chemisorptions [43]. Negative values obtained for maximum adsorption capacity of CWB reveals that adsorption of Pb, Mn and Cu onto CWB in the leachate does not follow Langmuir isotherm. In another study, negative values for adsorption capacity of dyes onto AC was obtained [35], which is practically and experimentally impossible. The highest value of the Langmuir constant b , 3.2 L mg^{-1} , was obtained for Pb adsorption onto PWB (Table 3) exhibiting greater affinity of Pb for the surface of PWB compared to Mn and Cu in landfill leachate. It seems that the monolayer adsorption capacity of Pb onto PWB provides a better fit to the experimental data compared to Mn and Cu. Experimental results showed that adsorbed amounts of the heavy metals on BC were clearly increased with rising adsorbent dosage. Figure 4 compares the simulated isotherm curves and measured data for adsorption of Pb, Mn and Cu onto BC based on Langmuir expression. Results indicated that Langmuir isotherm is unable to describe the equilibrium data perfectly in most cases.

379 3.4.2. *Linearized and non-linearized Freundlich isotherms*

380 The Freundlich isotherm has been widely applied to characterize the adsorption of organic
381 and inorganic pollutants using various adsorbents [44]. Freundlich isotherm constants found
382 through plotting $\ln q_e$ vs $\ln C_e$ are given in Table 4. The ratio of the amount of adsorbate
383 adsorbed onto a given mass of adsorbent to the adsorbate concentration in the solution using the
384 Freundlich model is represented by the following equation:

385
$$q_e = K_F C_e^{\frac{1}{n}} \quad (10)$$

386 Where, K_F is the Freundlich constant representing the relative adsorption intensity of the
387 adsorbent related to the bonding energy, and n is the heterogeneity factor indicating the deviation
388 from linearity of adsorption which is commonly known as Freundlich coefficient. Linearized
389 form of the Freundlich isotherm can be used to evaluate the adsorption data and determine the
390 Freundlich model constants as follows:

391
$$\ln q_e = \ln K_F + \frac{1}{n} \ln C_e \quad (11)$$

392 The corresponding coefficients of correlation for Freundlich model were found to be high
393 for adsorption of Pb, Mn, and Cu onto PWB and CWB (≥ 0.99) indicating a good linearity;
394 however, the values of Freundlich coefficient, n , did not fall within the favorable range for
395 CWB. Favorability of the Freundlich isotherm is generally indicated by the magnitude of the
396 exponent n . The values of n ranging from 2 to 10 is stated to represent a good fit, values ranging
397 from 1 to 2 indicates relatively difficult adsorption, and less than 1 shows poor adsorption
398 characteristics [45]. Acceptable adsorption characterized by values of n between 1 and 10 has
399 also been reported in the literature [21, 46]. The highest value of the Freundlich coefficient was
400 obtained for adsorption of Pb onto PWB ($n = 2.0$) (Table 4). Higher values of K_F were found for

401 adsorption of the heavy metals onto PWB indicating the greater relative adsorption capacity of
402 PWB compared to CWB to eliminate Pb, Mn, and Cu from the landfill leachate. Results show
403 that linearized Freundlich and Langmuir models could not adequately describe adsorption of Pb,
404 Mn, and Cu onto CWB in landfill leachate. In order to find the Freundlich maximum adsorption
405 capacity, q_m , it is necessary to keep the initial concentration of adsorbate constant and use the
406 variable dosage of adsorbent; that means $\ln q_m$ is the extrapolated value of $\ln q$ for $C = C_0$. Thus,
407 the Freundlich maximum adsorption capacity can be described as follows:

$$408 \quad q_m = K_F (C_0)^{\frac{1}{n}} \quad (12)$$

409 Where, q_m is the Freundlich maximum adsorption capacity (mg g^{-1}). The calculated
410 maximum adsorption capacity of PWB for Pb, Mn, and Cu using the Freundlich isotherm were
411 greater than the corresponding values for CWB, respectively, by a factor of 2.3, 5.3, and 1.4.
412 Comparing the maximum adsorption capacity produced by application of the Freundlich and
413 Langmuir-1 models reveals that predicted q_{max} using the Freundlich isotherm is markedly lower
414 than the corresponding values obtained by the Langmuir-1 expression for PWB.

415 It can be inferred from the Fig. 5a, 5b and 5c that the predicted adsorption capacity of PWB
416 and CWB using the linearized Freundlich isotherm is drastically underestimated for Pb, Mn and
417 Cu. Experimental data on adsorption of the heavy metals onto BC in landfill leachate also
418 suggest higher performance of PWB than CWB. Adsorbent particle size may considerably affect
419 removal of target contaminants from aqueous solutions. Higher effectiveness of PWB compared
420 to CWB in sorption of heavy metals in landfill leachate can also be attributed to the increased
421 internal surface area with decreasing BC particle size [47]. Smaller particle size provides high
422 capability of adsorption as a result of transfer of heavy metals through shorter pathways inside
423 the adsorbent particle pores [48]. In a previous study, Cr removal from an aqueous solution

424 declined from 70 to 14%, when the *Eucalyptus Camaldulensis* particle size increased from 0.063
425 to 2 mm [49], which is consistent with our findings. Higher BET surface area obtained for PWD
426 compared to CWB is another reason for higher adsorption efficiency and capacity of PWB, as
427 suggested in the literature [50].

428 Error analysis also indicates high values of SSE for linearized Freundlich isotherm. The SSE
429 values found for the Freundlich model are significantly higher than the obtained values for the
430 Langmuir model. Overally, results indicated no adequate agreement between the predicted and
431 measured adsorption data, implying the lack of validity of the linearized Freundlich isotherm to
432 model the adsorption of the heavy metals onto BC in the leachate. Both linear and non-linear
433 fitting of the experimental data to the Freundlich model yield high R^2 in most cases but the error
434 analysis presented a great difference between linear and non-linear fitting. The value of SSE
435 calculated for non-linear fitting was much lower than that obtained for linear fitting, as it could
436 also be realized by comparing experimental and modeled data presented in Fig. 5d, 5e and 5f.
437 Results indicate that non-linear fitting of the measured data to the Freundlich isotherm could
438 provide significantly more robust prediction compared to the linear fitting. However, the
439 obtained values for the constant n was less than 1 when CWB was used as an adsorbent both for
440 linear and non-linear fitting of data indicating unfavorable adsorption of Pb, Mn, and Cu onto
441 CWB. Results indicated much higher values of q_m when non-linearized regression was applied.
442 In other words, linearization of the Freundlich isotherm caused underestimation of q_m , while
443 fitting the measured data to non-linearized form of the Freundlich model depicted greater affinity
444 between the experimental and predicted data. Application of non-linear Freundlich isotherm
445 produced more valid data with significantly higher values of R^2 as well as much smaller SSE.
446 Overally, results indicated that linearization of the Freundlich isotherm to fit the experimental

447 data may generate higher errors and significantly deviate the predicted adsorption capacity of a
448 given adsorbent from the experimental data.

449 *3.4.3. Temkin isotherm*

450 Temkin isotherm equation contains a factor that reflects the adsorbent-adsorbate
451 interactions. The nonlinear form of Tempkin isotherm is represented by the following equation:

452
$$q_e = \frac{RT}{b_T} \ln(K_T C_e) \quad (13)$$

453 Where, T is the absolute temperature in Kelvin (K), R is the universal gas constant, 8.314 J
454 mol⁻¹ K⁻¹, b_T is the constant related to the heat of adsorption indicating the variation of
455 adsorption energy (J mol⁻¹), and K_T is the Temkin equilibrium binding constant (L g⁻¹)
456 corresponding to the maximum binding energy. The dimensionless term $(RT)/b_T$ can be
457 substituted by B_T , thus Temkin isotherm equation can be linearized as given by the following
458 equation:

459
$$q_e = B_T \ln K_T + B_T \ln C_e \quad (14)$$

460 The obtained parameters of Temkin model are given in Table 5. Values of R² found using
461 the linear transformation of the Temkin equation, were comparable to the non-linearized
462 Freundlich model. The variation of adsorption energy, b_T , was positive for all the studied heavy
463 metals implying that the adsorption of Pb, Mn and Cu onto BC is an exothermic reaction (22 kJ
464 mol⁻¹). Salam reported that the physical adsorption is characterized by adsorption energy in the
465 range of 5-40 kJ mol⁻¹ [5]. Physiosorption may occur as a result of weak forces of Van der Waals
466 between the adsorbates and adsorbents [12]. Higher amounts of variation of energy obtained
467 using the Temkin isotherm for adsorption of Pb, Mn, and Cu onto PWB relative to those
468 obtained for CWB indicates greater capacity of PWB to adsorb heavy metals in landfill leachate.
469 It should be noticed that the Temkin isotherm does not provide any estimation of the maximum

470 adsorption capacity of a given adsorbent. In spite of the non-linear Langmuir equation, if the
471 equilibrium concentration is increased, the adsorption capacity of the original Temkin equation,
472 q_e , does not converge to any limiting value. Figure 6 indicates that the predicted equilibrium
473 curves using Temkin model are very close to those obtained experimentally; however, deviation
474 of the predicted adsorption using the Temkin model slightly increased when lower dosage of BC
475 was applied. Error analysis indicates smaller values of the SSE relative to the Langmuir-1 and
476 linear Freundlich isotherms; however, the non-linear Freundlich model exhibited the lowest
477 values of SSE for adsorption of Pb, Mn and Cu onto BC in this study. Based on the obtained
478 results it seems that Temkin model can adequately describe the adsorption of the heavy metals
479 onto PWB and CWB in the leachate. Adsorption of Pb, Mn and Cu onto BC in landfill leachate
480 was adequately represented by the applied isotherm models, except the linear Freundlich model
481 implying that adsorption of heavy metals onto BC may be controlled by surface diffusion and
482 pore diffusion simultaneously as well as adsorption at an active preoccupied site. Overall,
483 results indicated promising removal of the heavy metals from landfill leachate using BC, which
484 could be well described by non-linearized Freundlich and Temkin models.

485 **4. Conclusions**

486 The present study aimed to assess the capability of BC in removal of Pb, Mn and Cu from
487 landfill leachate and model the adsorption kinetics and isotherms of the heavy metals onto BC.
488 Results indicated that the wood-derived BC is an effective adsorbent for the removal of Pb, Mn
489 and Cu from landfill leachate. The adsorption affinity of PWB for Pb, Mn, and Cu was greater
490 than CWB in all treatments. The contact times of 200 and 150 min were sufficient to reach
491 adsorption equilibrium condition, respectively for PWB and CWB. The removal efficiency of the
492 heavy metals only slightly enhanced as BC dosage exceeded 20 g L⁻¹. PWB showed the highest

493 experimental adsorption intensity of 1.58 mg g⁻¹ for the removal of Mn from the landfill
494 leachate. Beside BC particle size, other properties such as structural and pore space volume of
495 BC may also affect adsorption behavior of heavy metals in aqueous solutions, which is suggested
496 to be further investigated in future studies. The pseudo second-order kinetic model precisely
497 represented the adsorption kinetic data for BC suggesting the chemisorptions of Cd onto BC
498 particles. Calculated q_e using the Elovich kinetics model also agreed well with the experimental
499 q_e . Two distinct adsorption stages for the adsorption of the heavy metals onto BC in the leachate
500 was clearly observed; first the migration of metals from the leachate system to the external
501 surface of BC during which the mass transfer is very rapid and physical processes control the
502 adsorption, followed by the prolonged intra-particle diffusion characterized by slow adsorption.
503 The non-linear Freundlich isotherm best describes the equilibrium adsorption data, followed by
504 the Temkin isotherm. Linearized Freundlich model could only moderately describe adsorption of
505 the heavy metals onto PWB, while it was not able to represent the adsorption by CWB.
506 Linearization method for the Langmuir isotherm also affects the error structure suggesting that
507 the linearization of non-linear isotherm models may violate the theory behind an isotherm and
508 alter error distribution. It is recommended to use wood-derived BC as an effective adsorbent to
509 remove heavy metals from landfill leachate.

510

511 **Availability of data and materials**

512 All data generated or analyzed during this study are included within the article.

513 **Competing interests**

514 The authors declare they have no competing interests.

515 **Funding**

516 This work was supported by University of Tehran.

517 **Authors' contributions**

518 Ali Daryabeigi Zand (ADZ) was responsible for developing the theory and idea, carrying out the
519 experiments, performing and verifying the analytic calculations and numerical simulations, and
520 writing the manuscript. Maryam Rabiee Abyaneh (MRA) was responsible for carrying out the
521 experiments, performing the analytic calculations and numerical simulations, and writing the
522 manuscript.

523 **Acknowledgments**

524 The authors would like to thank the University of Tehran for the support. The first author would
525 also like to sincerely thank the Labor of Applied Geosciences, University of Tübingen, Germany,
526 for the skilled laboratory support.

527 **References**

- 528 1. Phan TN, Van Truong TT, Ha NB, Nguyen PD, Bui XT, Dang BT, et al. High rate nitrogen
529 removal by ANAMMOX internal circulation reactor (IC) for old landfill leachate treatment.
530 Bioresour Technol. 2017;234:281–8.
- 531 2. Poblete R, Oller I, Maldonado MI, Luna Y, Cortes E. Cost estimation of COD and color
532 removal from landfill leachate using combined coffee-waste based activated carbon with
533 advanced oxidation processes. J Environ Chem Eng. 2017;5:114–21.
- 534 3. Xu J, Long YY, Shen DS, Feng HJ, Chen T. Optimization of Fenton treatment process for
535 degradation of refractory organics in pre-coagulated leachate membrane concentrates. J
536 Hazard Mater. 2017;323:674–80.
- 537 4. Dan A, Oka M, Fujii Y, Soda S, Ishigaki T, Machimura T, et al. Removal of heavy metals
538 from synthetic landfill leachate in lab-scale vertical flow constructed wetlands. Sci Total
539 Environ. 2017;584–5:742–50.

- 540 5. Salam MA. Removal of heavy metal ions from aqueous solutions with multi-walled carbon
541 nanotubes: kinetic and thermodynamic studies. *Int J Environ Sci Te.* 2013;10:677–88.
- 542 6. Erabee IK, Ahsan A, Jose B, Aziz MMA, Ng AWM, Idrus S, et al. Adsorptive treatment of
543 landfill leachate using activated carbon modified with three different methods. *KSCE J Civ*
544 *Eng.* 2018;22:1083–95.
- 545 7. Foo KY, Hameed BH. An overview of landfill leachate treatment via activated carbon
546 adsorption process. *J Hazard Mater.* 2009;171:54–60.
- 547 8. Beesley L, Moreno-Jimenez E, Gomez-Eyles JL, Harris E, Robinson B, Sizmur T. A review
548 of biochars' potential role in the remediation, revegetation and restoration of contaminated
549 soils. *Environ Pollut.* 2011;159:3269–82.
- 550 9. Issabayeva G, Aroua MK, Sulaiman NM. Study on palm shell activated carbon adsorption
551 capacity to remove copper ions from aqueous solutions. *Desalination.* 2010;262:94–8.
- 552 10. Wong S, Ngadi N, Inuwa IM, Hassan O. Recent advances in applications of activated
553 carbon from biowaste for wastewater treatment: a short review. *J Clean Prod.*
554 2018;175:361–75.
- 555 11. Soco E, Kalembkiewicz J. Adsorption of nickel(II) and copper(II) ions from aqueous
556 solution by coal fly ash. *J Environ Chem Eng.* 2013;1:581–8.
- 557 12. Itodo AU, Itodo HU, Gafar MK. Estimation of specific surface area using Langmuir
558 isotherm method. *J Appl Sci Environ Manage.* 2011;14:141–5.
- 559 13. Shehzad A, Bashir MJK, Sethupathi S, Lim JW. An insight into the remediation of highly
560 contaminated landfill leachate using sea mango based activated bio-char: optimization,
561 isothermal and kinetic studies. *Desalin Water Treat.* 2016;57:22244–57.
- 562 14. Kavitha D, Namasivayam C. Experimental and kinetic studies on methylene blue adsorption

- 563 by coir pith carbon. *Bioresour Technol.* 2007;98:14–21.
- 564 15. Regazzoni AE. Adsorption kinetics at solid/aqueous solution interfaces: on the boundaries
565 of the pseudo-second order rate equation. *Colloid Surface A* 2020;585:124093.
- 566 16. Tofighy MA, Mohammadi T. Adsorption of divalent heavy metal ions from water using
567 carbon nanotube sheets. *J Hazard Mater.* 2011;185:140–7.
- 568 17. Largitte L, Pasquier R. A review of the kinetics adsorption models and their application to
569 the adsorption of lead by an activated carbon. *Chem Eng Res Des.* 2016;109:495–504.
- 570 18. Pandiarajan A, Kamaraj R, Vasudevan S, Vasudevan S. OPAC (orange peel activated
571 carbon) derived from waste orange peel for the adsorption of chlorophenoxyacetic acid
572 herbicides from water: adsorption isotherm, kinetic modelling and thermodynamic studies.
573 *Bioresour Technol.* 2018;261:329–41.
- 574 19. Malwade K, Lataye D, Mhaisalkar V, Kurwadkar S, Ramirez D. Adsorption of hexavalent
575 chromium onto activated carbon derived from *Leucaena leucocephala* waste sawdust:
576 kinetics, equilibrium and thermodynamics. *Int J Environ Sci Te.* 2016;13:2107–16.
- 577 20. Balarak D, Mostafapour FK, Azarpira H, Joghataei A. Langmuir, Freundlich, Temkin and
578 Dubinin–Radushkevich isotherms studies of equilibrium sorption of ampicilin unto
579 montmorillonite nanoparticles. *Brit J Pharm Res.* 2017;20:1–9.
- 580 21. Igwe JC, Abia AA. Adsorption isotherm studies of Cd (II), Pb (II) and Zn (II) ions
581 bioremediation from aqueous solution using unmodified and EDTA-modified maize cob.
582 *Eclet Quím.* 2007;32:33–42.
- 583 22. Qambrani NA, Rahman MM, Won S, Shim S, Ra C. Biochar properties and eco-friendly
584 applications for climate change mitigation, waste management, and wastewater treatment: a
585 review. *Renew SustEnerg Rev.* 2017;79:255–73.

- 586 23. de Caprariis B, De Filippis P, Hernandez AD, Petrucci E, Petrullo A, Scarsella M, et al.
587 Pyrolysis wastewater treatment by adsorption on biochars produced by poplar biomass. *J*
588 *Environ Manage.* 2017;197:231–8.
- 589 24. Agraftioti E, Kalderis D, Diamadopoulos E. Arsenic and chromium removal from water
590 using biochars derived from rice husk, organic solid wastes and sewage sludge. *J Environ*
591 *Manage.* 2014;133:309–14.
- 592 25. Chen BL, Yuan MX. Enhanced sorption of polycyclic aromatic hydrocarbons by soil
593 amended with biochar. *J Soil Sediment.* 2011;11:62–71.
- 594 26. Marchal G, Smith KEC, Rein A, Winding A, de Jonge LW, Trapp S, et al. Impact of
595 activated carbon, biochar and compost on the desorption and mineralization of
596 phenanthrene in soil. *Environ Pollut.* 2013;181:200–10.
- 597 27. Pazoki M, Abdoli MA, Karbassi AR, Mehrdadi N, Yaghmaeian K. Attenuation of
598 municipal landfill leachate through land treatment. *J Environ Health Sci.* 2014;12:12.
- 599 28. Baird RB, Eaton AD, Rice EW, editors. Standard methods for the examination of water and
600 wastewater. 23rd ed. Washington, DC: American Public Health Association; 2017.
- 601 29. USEPA. SW-846 test method 3005A: acid digestion of waters for total recoverable or
602 dissolved metals for analysis by flame atomic absorption (FLAA) or inductively coupled
603 plasma (ICP) spectroscopy. Washington, DC: US Environmental Protection Agency; 1992.
- 604 30. Xue Q, Li JS, Wang P, Liu L, Li ZZ. Removal of heavy metals from landfill leachate using
605 municipal solid waste incineration fly ash as adsorbent. *Clean-Soil Air Water.*
606 2014;42:1626–31.
- 607 31. Singh B, Dolk MM, Shen QH, Camps-Arbestain M. Biochar pH, electrical conductivity and
608 liming potential. In: Singh B, Camps-Arbestain M, Lehmann J, editors. Biochar: a guide to

- analytical methods. Clayton South: Csiro Publishing; 2017. p. 23–38.
32. Qiu YP, Zheng ZZ, Zhou ZL, Sheng GD. Effectiveness and mechanisms of dye adsorption on a straw-based biochar. *Bioresour Technol*. 2009;100:5348–51.
33. Bogusz A, Oleszczuk P, Dobrowolski R. Adsorption and desorption of heavy metals by the sewage sludge and biochar-amended soil. *Environ Geochem Hlth*. 2019;41:1663–74.
34. Nagy B, Manzatu C, Maicaneanu A, Indolean C, Lucian BT, Majdik C. Linear and nonlinear regression analysis for heavy metals removal using *Agaricusbisporusmacrofungus*. *Arab J Chem*. 2017;10:S3569–79.
35. Kumar KV. Linear and non-linear regression analysis for the sorption kinetics of methylene blue onto activated carbon. *J Hazard Mater*. 2006;137:1538–44.
36. Idris S, Iyaka YA, Ndamitso MM, Mohammed EB, Umar MT. Evaluation of kinetic models of copper and lead uptake from dye wastewater by activated pride of barbados shell. *Am J Chem*. 2011;1:47–51.
37. Krishnan KA, Sreejalekshmi KG, Baiju RS. Nickel(II) adsorption onto biomass based activated carbon obtained from sugarcane bagasse pith. *Bioresour Technol*. 2011;102:10239–47.
38. Tagavifar M, Jang SH, Sharma H, Wang D, Chang LY, Mohanty K, et al. Effect of pH on adsorption of anionic surfactants on limestone: experimental study and surface complexation modeling. *Colloid Surface A*. 2018;538:549–58.
39. Ngah WSW, Kamari A, Koay Y. Equilibrium and kinetics studies of adsorption of copper(II) on chitosan and chitosan/PVA beads. *Int J Biol Macromol*. 2004;34:155–61.
40. Langmuir I. The adsorption of gases on plane surfaces of glass, mica and platinum. *J Am Chem Soc*. 1918;40:1361–403.

- 632 41. Hamdaoui O, Naffrechoux E. Modeling of adsorption isotherms of phenol and
633 chlorophenols onto granular activated carbon - Part II. Models with more than two
634 parameters. *J Hazard Mater.* 2007;147:401–11.
- 635 42. Hall KR, Eagleton LC, Acrivos A, Vermeulen T. Pore- and solid-diffusion kinetics in fixed-
636 bed adsorption under constant-pattern conditions. *Ind Eng Chem Fund.* 1966;5:212–23.
- 637 43. Kizito S, Wu SB, Kirui WK, Lei M, Lu QM, Bah H, et al. Evaluation of slow pyrolyzed
638 wood and rice husks biochar for adsorption of ammonium nitrogen from piggery manure
639 anaerobic digestate slurry. *Sci Total Environ.* 2015;505:102–12.
- 640 44. El-Aila HJ, Elsousy KM, Hartany KA. Kinetics, equilibrium, and isotherm of the adsorption
641 of cyanide by MDFSD. *Arab J Chem.* 2016;9:S198–203.
- 642 45. Elbana TA, Selim HM, Akrami N, Newman A, Shaheen SM, Rinklebe J. Freundlich
643 sorption parameters for cadmium, copper, nickel, lead, and zinc for different soils: influence
644 of kinetics. *Geoderma.* 2018;324:80–8.
- 645 46. Stromer BS, Woodbury B, Williams CF. Tylosin sorption to diatomaceous earth described
646 by Langmuir isotherm and Freundlich isotherm models. *Chemosphere.* 2018;193:912–20.
- 647 47. Al-Anber MA. Thermodynamics approach in the adsorption of heavy metals. In: Moreno
648 Pirajan JC, editor. *Thermodynamics – interaction studies – solids, liquids and gases.*
649 London: IntechOpen; 2011.
- 650 48. Al-Anber MA. Removal of high-level Fe³⁺ from aqueous solution using natural inorganic
651 materials: bentonite (NB) and quartz (NQ). *Desalination.* 2010;250:885–91.
- 652 49. Gebretsadik H, Gebrekidan A, Demlie L. Removal of heavy metals from aqueous solutions
653 using *Eucalyptus Camaldulensis*: an alternate low cost adsorbent. *Cogent Chem.*
654 2020;6:1720892.

655 50. Akpomie KG, Dawodu FA, Adebawale KO. Mechanism on the sorption of heavy metals
656 from binary-solution by a low cost montmorillonite and its desorption potential. Alex Eng J.
657 2015;54:757–67.

658

659

660 **Table 1.** Kinetic parameters of the pseudo second-order model for adsorption of heavy metals
 661 onto BC in landfill leachate

Adsorbate	BC dosage	Pseudo second-order kinetic for PWB				Pseudo second-order kinetic for CWB			
		$q_{e(\text{cal.})}$ (mg g ⁻¹)	k_{2p}	R^2	SSE	$q_{e(\text{cal.})}$ (mg g ⁻¹)	k_{2p}	R^2	SSE
Pb	0.05	0.45	0.12	0.999	0.000	0.36	0.15	0.999	0.000
	0.1	0.44	0.12	0.999	0.000	0.35	0.15	0.999	0.000
	0.25	0.34	0.15	0.999	0.000	0.27	0.20	0.999	0.000
	0.5	0.27	0.19	0.999	0.000	0.19	0.28	0.999	0.000
	0.75	0.21	0.24	0.999	0.000	0.15	0.36	0.999	0.000
	1	0.17	0.31	0.999	0.000	0.12	0.47	0.999	0.000
	1.5	0.12	0.43	0.999	0.000	0.09	0.63	0.999	0.000
	2	0.09	0.56	0.999	0.000	0.07	0.79	0.999	0.000
	3	0.07	0.81	0.999	0.000	0.05	1.10	0.999	0.000
	5	0.04	1.39	0.999	0.000	0.03	1.75	0.999	0.000
Mn	0.05	1.62	0.03	0.999	0.001	1.40	0.04	0.999	0.001
	0.1	1.54	0.03	0.999	0.000	1.40	0.04	0.999	0.001
	0.25	1.10	0.05	0.999	0.000	0.97	0.06	0.999	0.000
	0.5	0.85	0.06	0.999	0.000	0.73	0.07	0.999	0.000
	0.75	0.69	0.07	0.999	0.000	0.58	0.09	0.999	0.000
	1	0.56	0.09	0.999	0.000	0.47	0.12	0.999	0.000
	1.5	0.43	0.12	0.999	0.000	0.36	0.16	0.999	0.000
	2	0.34	0.15	0.999	0.000	0.28	0.20	0.999	0.000
	3	0.24	0.22	0.999	0.000	0.20	0.28	0.999	0.000
	5	0.15	0.35	0.999	0.000	0.13	0.45	0.999	0.000
Cu	0.05	0.40	0.13	0.999	0.000	0.46	0.11	0.999	0.000
	0.1	0.39	0.13	0.999	0.000	0.43	0.12	0.999	0.000
	0.25	0.33	0.16	0.999	0.000	0.32	0.17	0.999	0.000
	0.5	0.26	0.20	0.999	0.000	0.24	0.23	0.999	0.000
	0.75	0.22	0.24	0.999	0.000	0.18	0.29	0.999	0.000
	1	0.17	0.29	0.999	0.000	0.16	0.37	0.999	0.000
	1.5	0.13	0.38	0.999	0.000	0.12	0.49	0.999	0.000
	2	0.11	0.49	0.999	0.000	0.09	0.62	0.999	0.000
	3	0.08	0.70	0.999	0.000	0.07	0.87	0.999	0.000
	5	0.05	1.09	0.999	0.000	0.04	1.38	0.999	0.000

662
663

664

665 **Table 2.** Kinetic parameters of the Elovich model for adsorption of heavy metals onto BC in
 666 landfill leachate

Adsorbate	Adsorbent dosage	Elovich kinetics for PWB					Elovich kinetics for CWB				
		$q_{e(cal.)}$ (mg g ⁻¹)	β	α	R^2	SSE	$q_{e(cal.)}$ (mg g ⁻¹)	β	α	R^2	SSE
Pb	0.05	0.49	14.5	0.056	0.953	0.002	0.39	18.2	0.044	0.955	0.001
	0.1	0.48	14.7	0.055	0.952	0.002	0.38	18.5	0.043	0.956	0.001
	0.25	0.37	18.9	0.043	0.948	0.002	0.30	23.8	0.034	0.955	0.001
	0.5	0.30	23.8	0.034	0.948	0.001	0.21	34.5	0.024	0.955	0.000
	0.75	0.23	30.3	0.027	0.949	0.001	0.16	43.5	0.019	0.955	0.000
	1	0.18	38.5	0.021	0.937	0.000	0.13	52.6	0.015	0.951	0.000
	1.5	0.13	52.6	0.015	0.937	0.000	0.10	71.4	0.011	0.951	0.000
	2	0.10	71.4	0.011	0.937	0.000	0.08	90.9	0.009	0.951	0.000
	3	0.07	100.0	0.008	0.939	0.000	0.06	125.0	0.006	0.951	0.000
	5	0.04	166.7	0.005	0.935	0.000	0.04	200.0	0.004	0.952	0.000
Mn	0.05	1.76	4.0	0.201	0.952	0.032	1.55	4.6	0.176	0.956	0.028
	0.1	1.71	4.1	0.195	0.952	0.031	1.53	4.6	0.174	0.956	0.026
	0.25	1.20	5.9	0.137	0.948	0.016	1.07	6.6	0.121	0.955	0.013
	0.5	0.84	8.6	0.107	0.948	0.000	0.81	8.8	0.092	0.955	0.008
	0.75	0.76	9.3	0.086	0.948	0.006	0.63	11.1	0.072	0.954	0.005
	1	0.61	11.5	0.07	0.937	0.004	0.52	13.6	0.059	0.95	0.003
	1.5	0.47	15.2	0.053	0.937	0.002	0.38	18.9	0.045	0.95	0.001
	2	0.37	18.9	0.043	0.937	0.002	0.31	22.8	0.035	0.95	0.001
	3	0.26	27.0	0.03	0.936	0.001	0.23	31.3	0.026	0.95	0.001
	5	0.16	43.5	0.019	0.936	0.000	0.14	50.0	0.016	0.95	0.000
Cu	0.05	0.45	15.9	0.051	0.952	0.003	0.51	13.9	0.058	0.957	0.003
	0.1	0.44	16.1	0.050	0.952	0.003	0.47	15.2	0.053	0.957	0.002
	0.25	0.35	20.0	0.041	0.948	0.001	0.35	20.0	0.041	0.955	0.001
	0.5	0.28	25.0	0.032	0.948	0.001	0.26	27.0	0.030	0.955	0.001
	0.75	0.23	30.3	0.027	0.948	0.000	0.20	35.8	0.023	0.954	0.000
	1	0.19	37.0	0.022	0.937	0.000	0.17	41.7	0.019	0.955	0.000
	1.5	0.14	50.0	0.016	0.937	0.000	0.13	55.6	0.014	0.955	0.000
	2	0.11	62.5	0.013	0.937	0.000	0.10	71.4	0.011	0.949	0.000
	3	0.08	90.9	0.009	0.936	0.000	0.07	100.0	0.008	0.949	0.000
	5	0.05	142.9	0.006	0.937	0.000	0.04	166.7	0.005	0.948	0.000

667
668

669 **Table 3.** Parameters of the Langmuir isotherm for adsorption of Pb, Mn and Cu onto BC in
 670 landfill leachate

Langmuir isotherm-type 1	Pb PWB	CWB	Mn PWB	CWB	Cu PWB	CWB
q_m (mg g ⁻¹)	0.44	-0.22	5.60	-0.65	5.90	-0.21
b (L mg ⁻¹)	3.22	-0.46	0.05	-0.12	0.04	-0.37
R^2	0.985	0.965	0.993	0.944	0.994	0.944
R_L	0.14	8.86	0.70	23.05	0.92	18.28
SSE	0.016	0.364	0.045	9.593	0.008	0.842

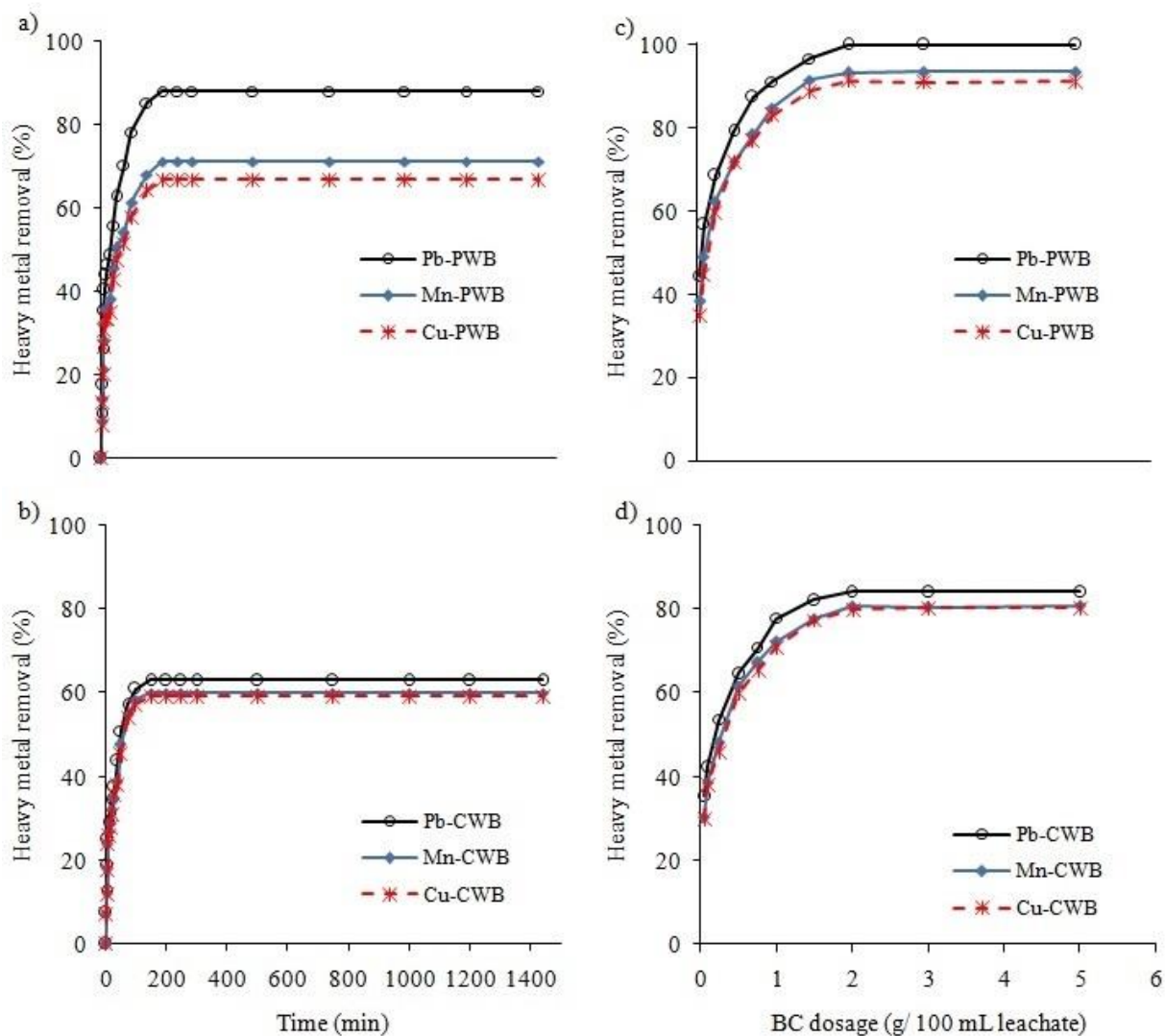
671
 672 **Table 4.** Linearized and non-linearized Freundlich isotherm constants for adsorption of Pb, Mn
 673 and Cu onto BC

Isotherm	Parameters	Pb PWB	CWB	Mn PWB	CWB	Cu PWB	CWB
Linearized	K _F	0.09	0.02	0.06	0.00	0.02	0.01
Freundlich	n	1.99	0.74	1.14	0.67	1.11	0.67
Isotherm	R^2	0.994	0.994	0.992	0.990	0.991	0.991
	q_{max}	0.12	0.05	0.34	0.06	0.06	0.04
	SSE	0.374	0.312	5.086	5.536	0.446	0.528
Non-linearized	K _F	0.34	0.19	0.28	0.91	0.20	0.14
Freundlich	n	2.03	0.81	1.11	0.72	1.22	0.71
Isotherm	R^2	0.967	0.990	0.988	0.989	0.993	0.998
	q_{max}	0.47	0.42	1.75	1.65	0.43	0.53
	SSE	0.0064	0.0012	0.0281	0.0216	0.0009	0.0004

674
 675
 676 **Table 5.** Temkin isotherm parameters for adsorption of Pb, Mn and Cu onto BC in the leachate

Temkin isotherm parameters	Pb PWB	CWB	Mn PWB	CWB	Cu PWB	CWB
b _T	0.11	0.19	0.54	0.82	0.15	0.27
K _T	22.3	3.2	1.8	0.7	4.6	2.0
R^2	0.964	0.935	0.889	0.930	0.958	0.938
SSE	0.004	0.008	0.262	0.131	0.006	0.018

677
 678
 679

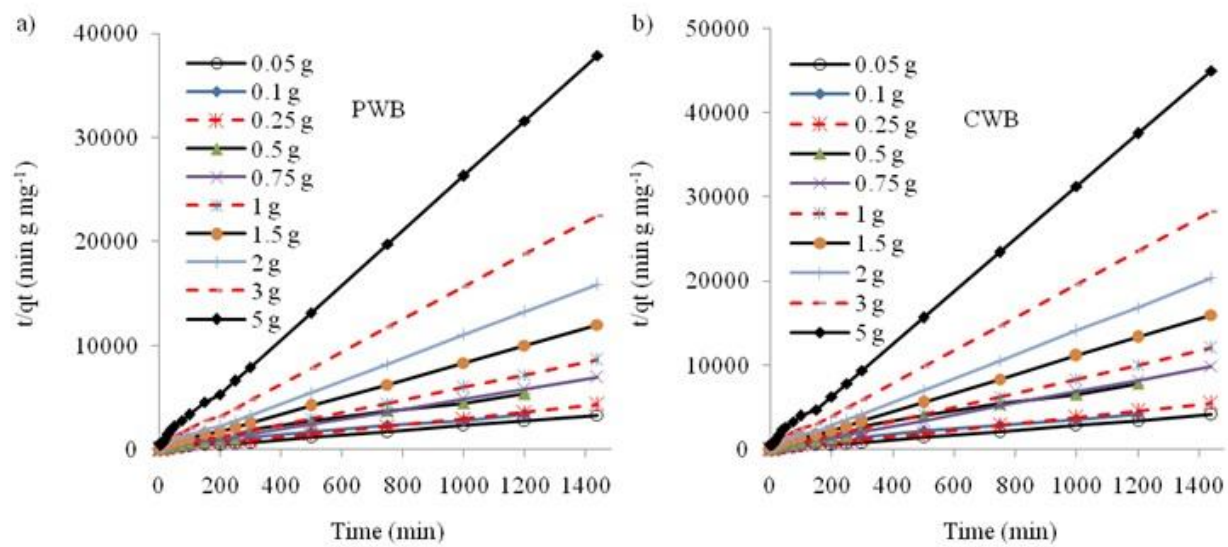


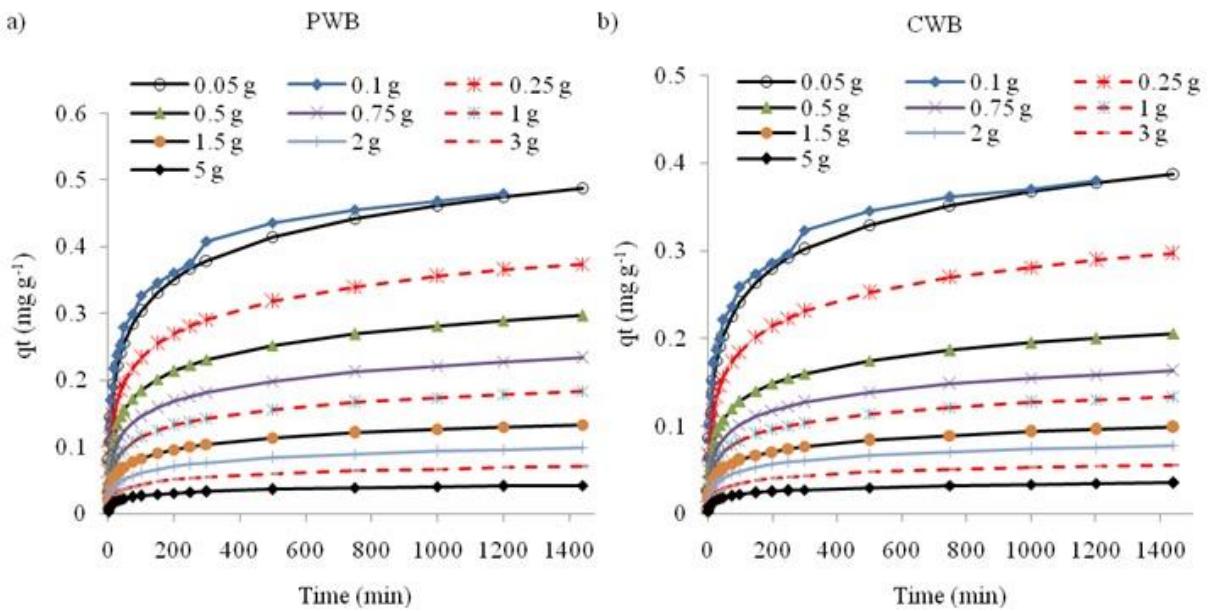
680

681 **Fig. 1.** Effect of contact time and biochar dosage on removal of heavy metals from landfill
 682 leachate

683

684

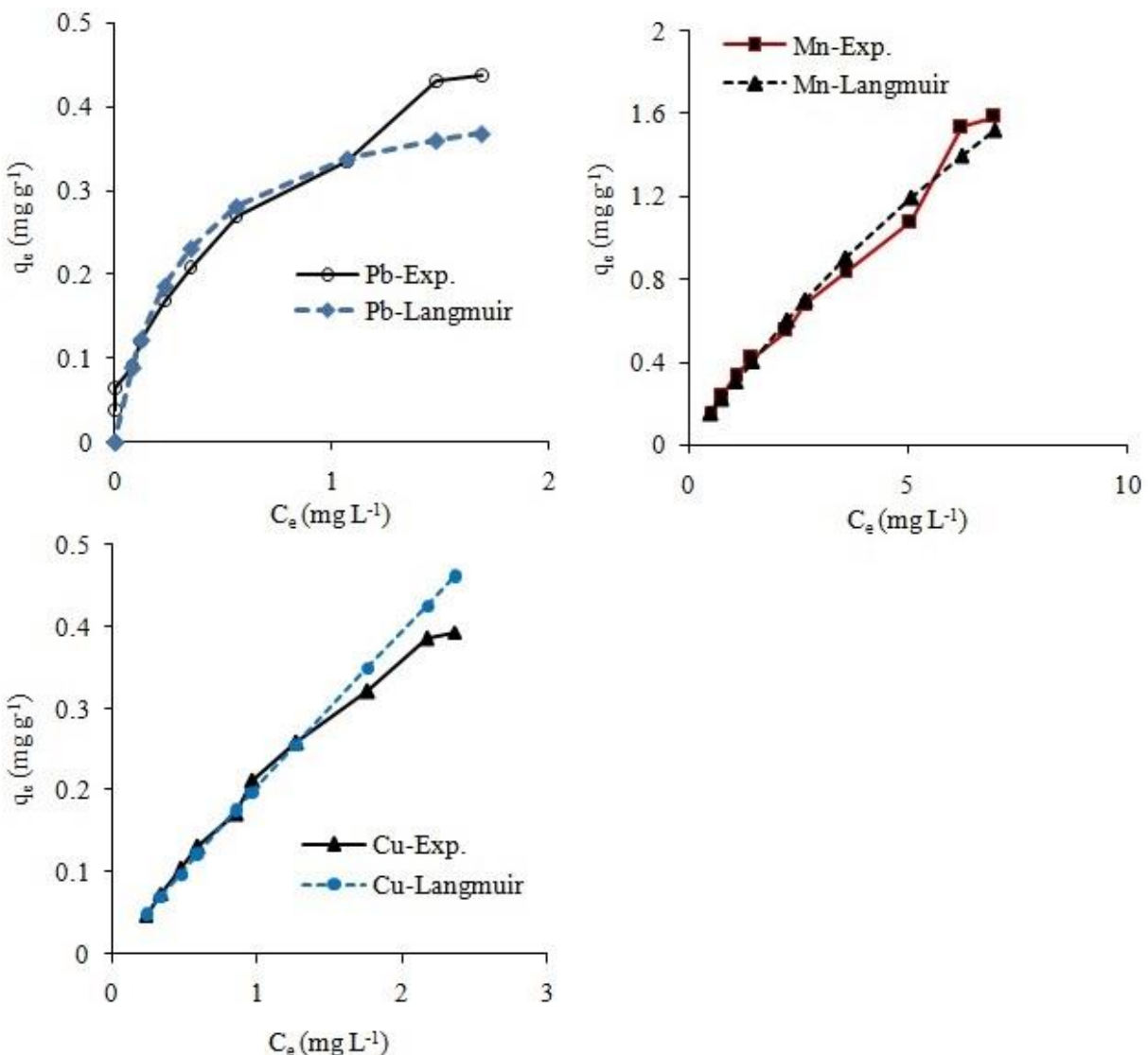
687 **Fig. 2.** Linearized pseudo second-order kinetics for adsorption of Pb onto PWB (a) and CWB (b)



689

690 **Fig. 3.** Determined quantities of adsorption capacity of Pb onto PWB (a) and CWB (b) using the
691 Elovich kinetic model

692

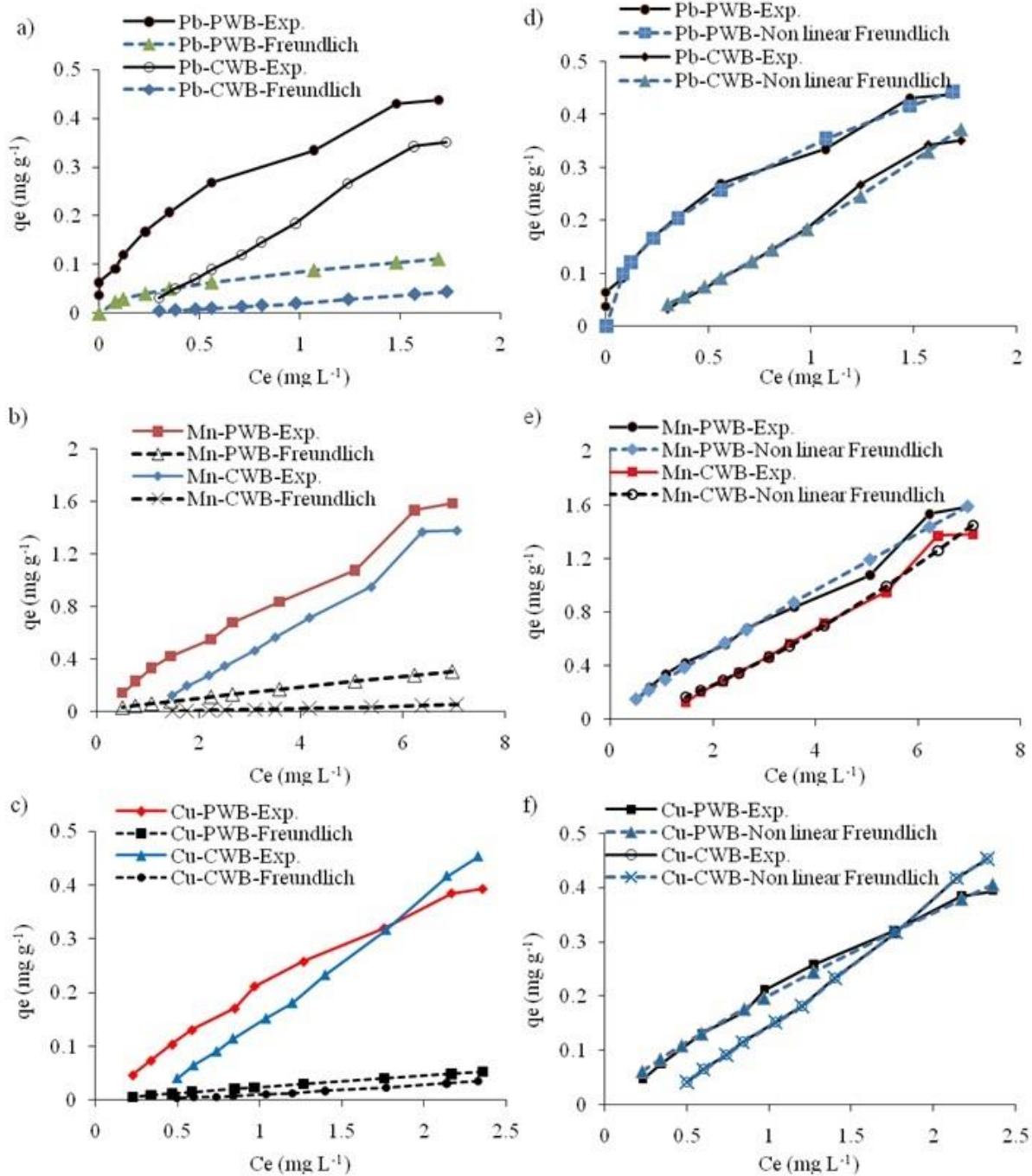


693

694 **Fig. 4.** Experimental and predicted adsorption of the heavy metals onto PWB in landfill leachate
695 using Langmuir-1 expression

696

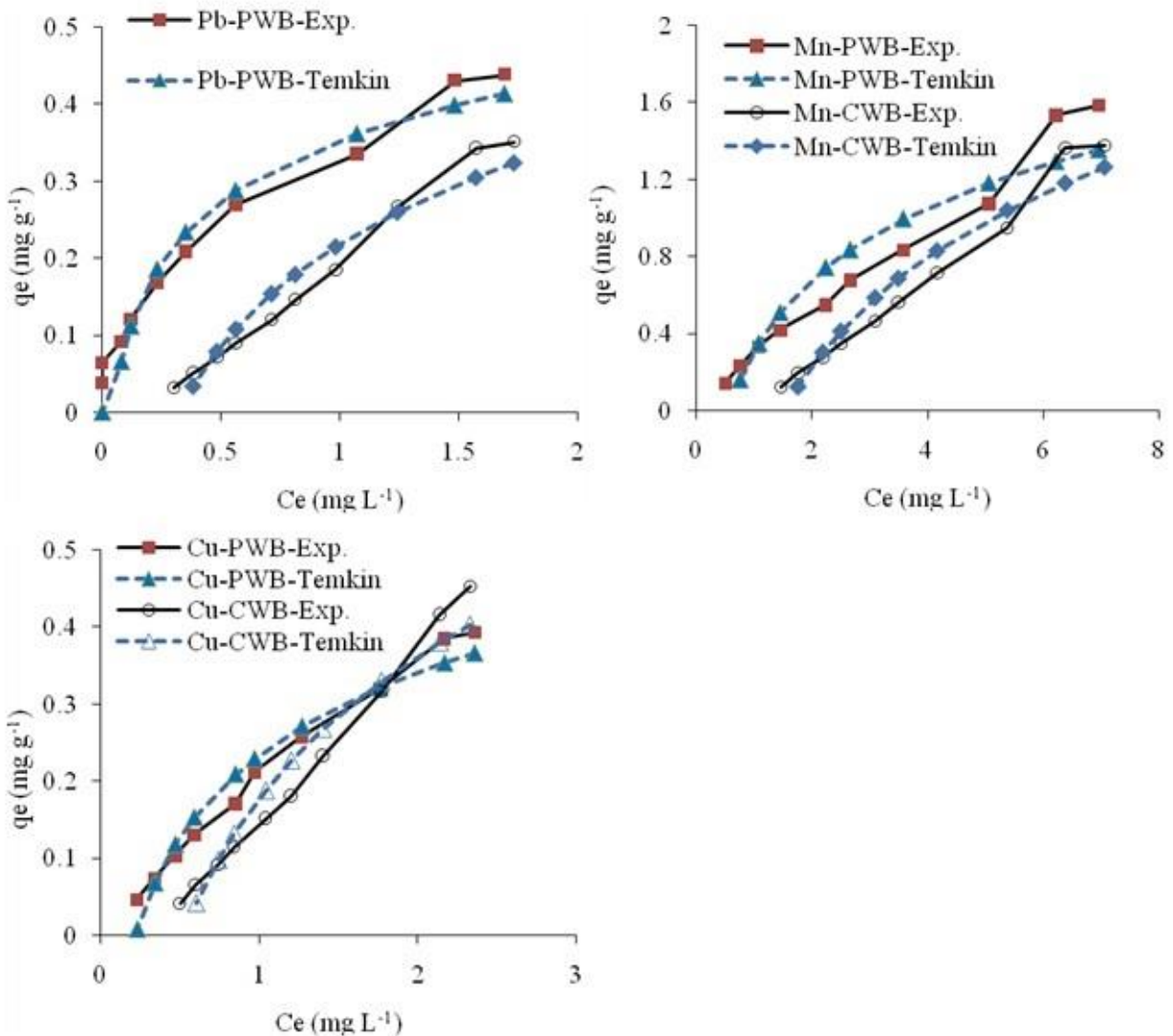
697



698

699 **Fig. 5.** Experimental and predicted adsorption of the heavy metals in leachate onto PWB and
700 CWB using linearized and non-linearized Freundlich equations

701



702

703 **Fig. 6.** Experimental and predicted adsorption of the heavy metals in landfill leachate onto PWB

704 and CWB using Temkin equation

705

Figures

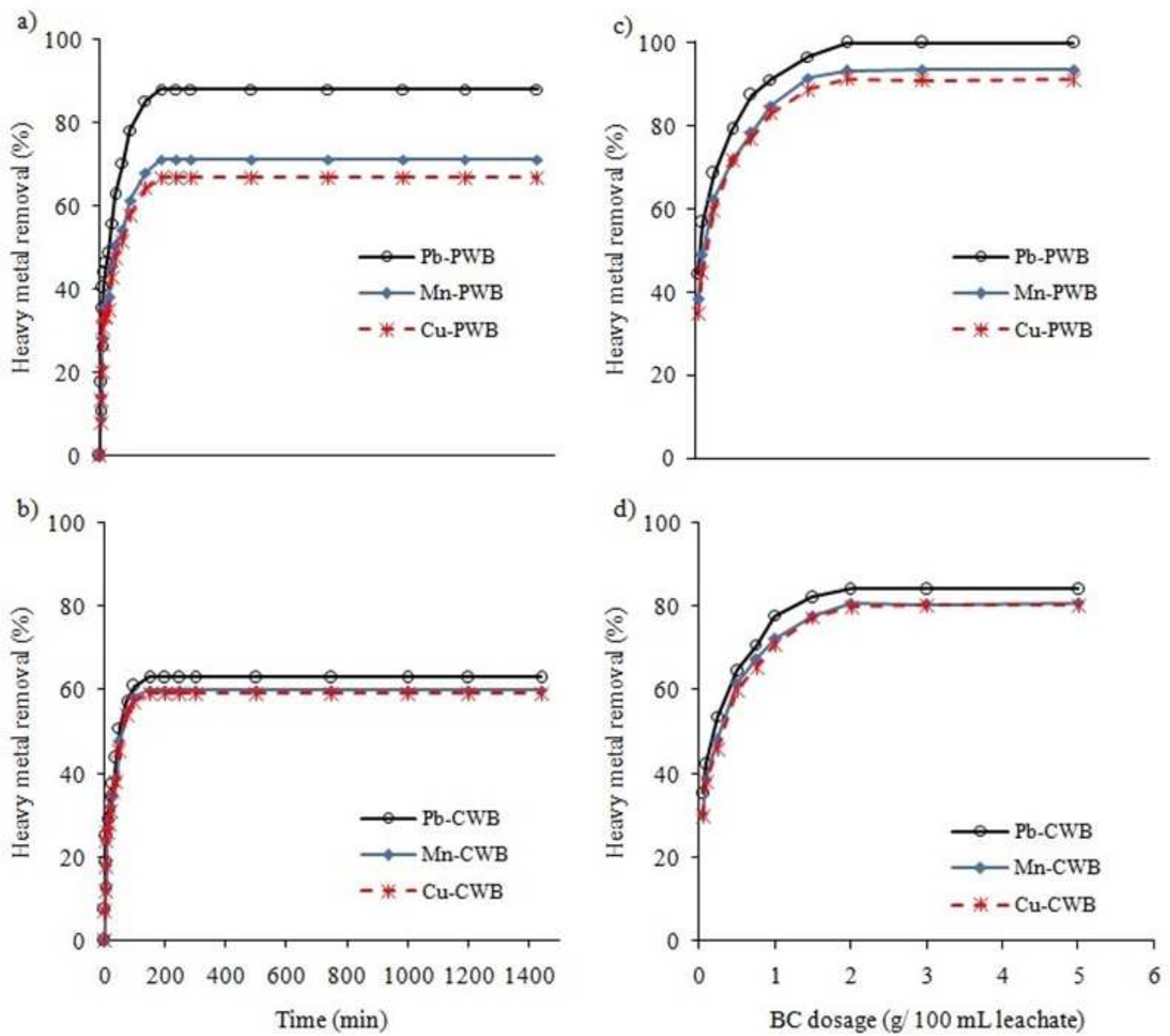


Figure 1

Effect of contact time and biochar dosage on removal of heavy metals from landfill leachate

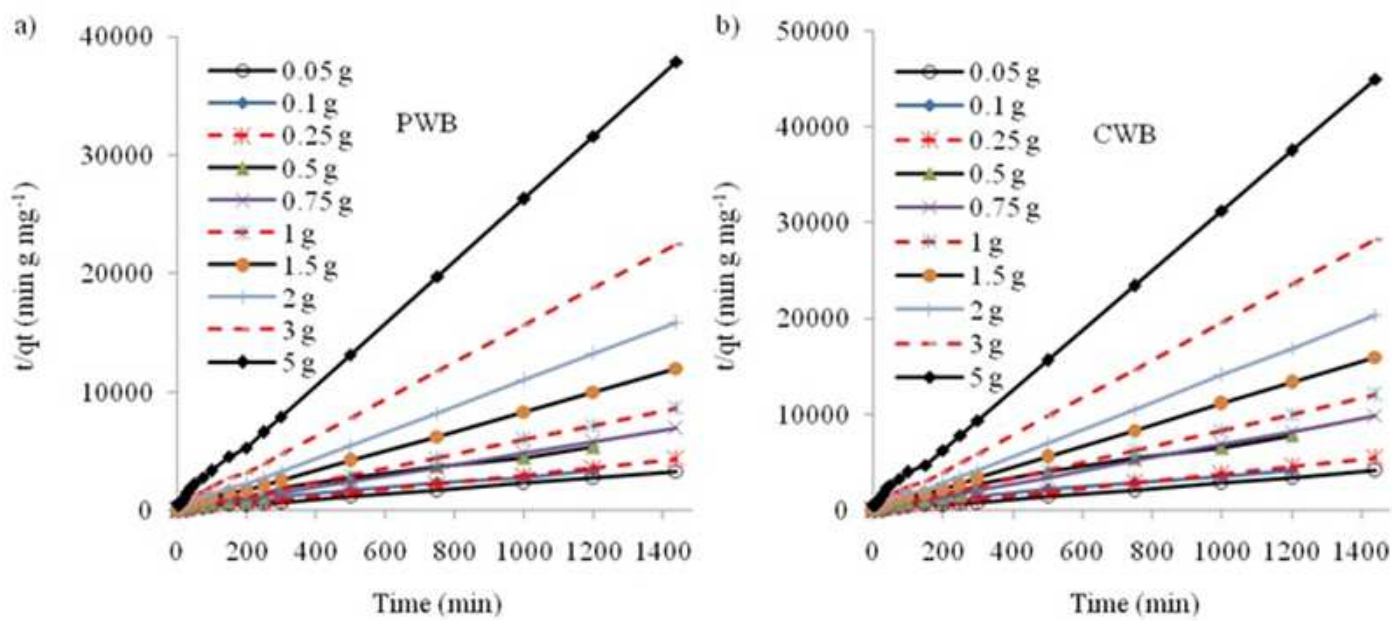


Figure 2

Linearized pseudo second-order kinetics for adsorption of Pb onto PWB (a) and CWB (b)

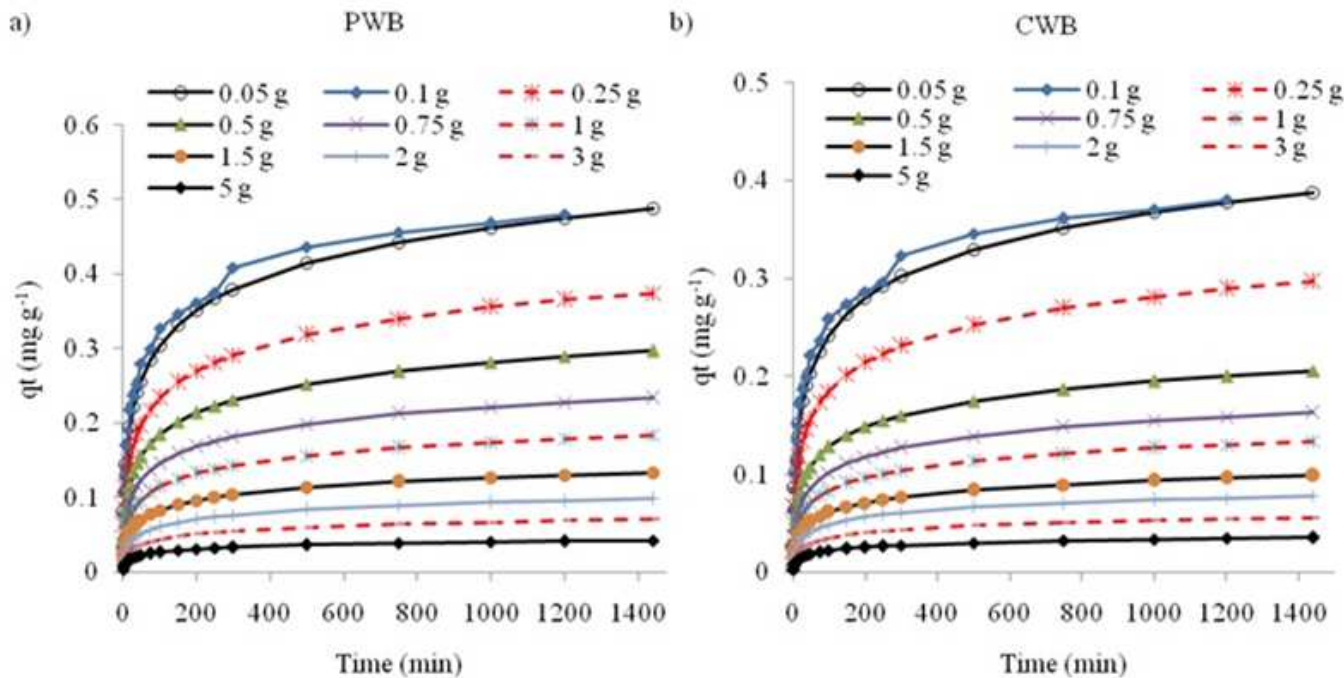


Figure 3

Determined quantities of adsorption capacity of Pb onto PWB (a) and CWB (b) using the Elovich kinetic model

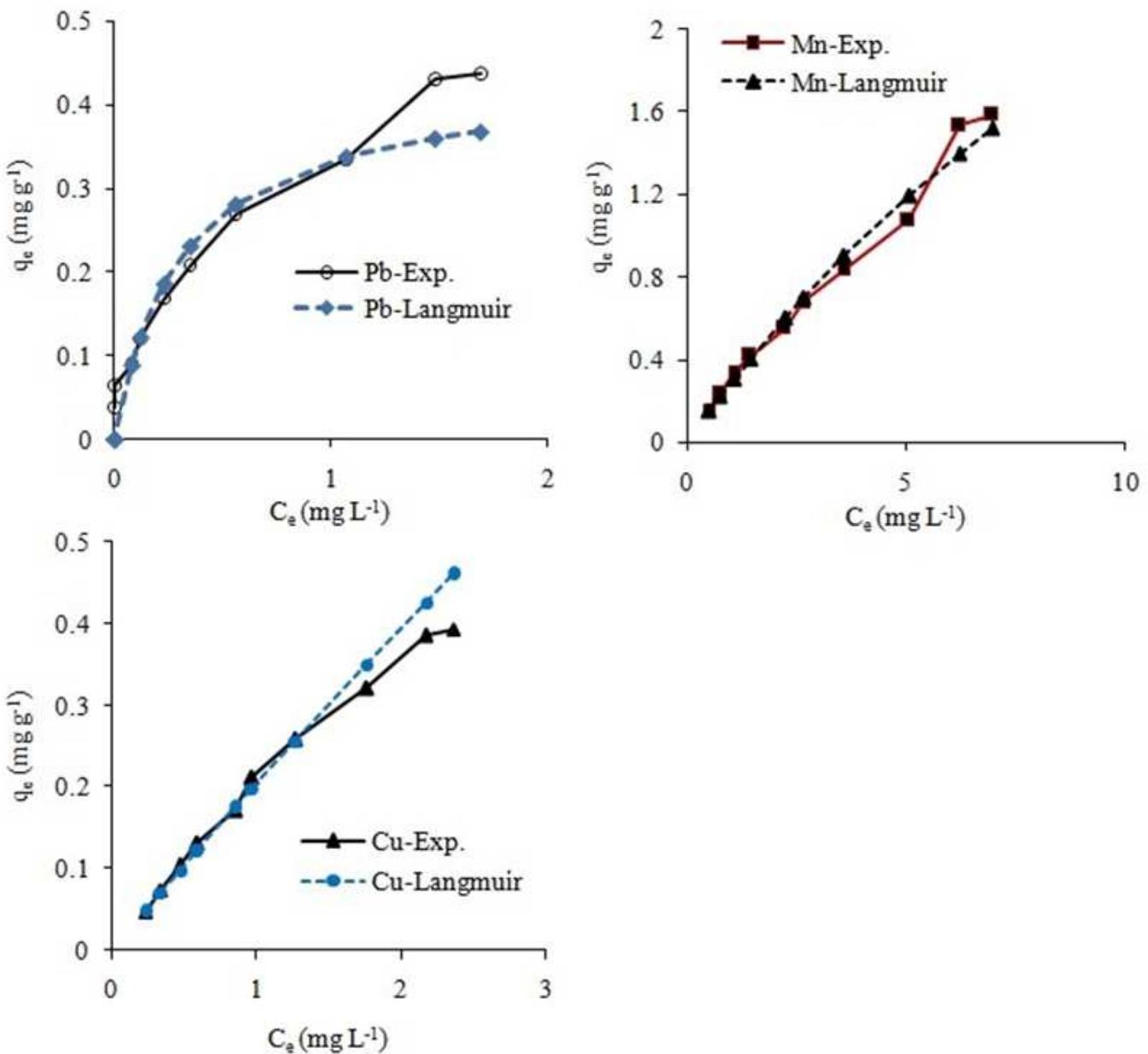


Figure 4

Experimental and predicted adsorption of the heavy metals onto PWB in landfill leachate using Langmuir-1 expression

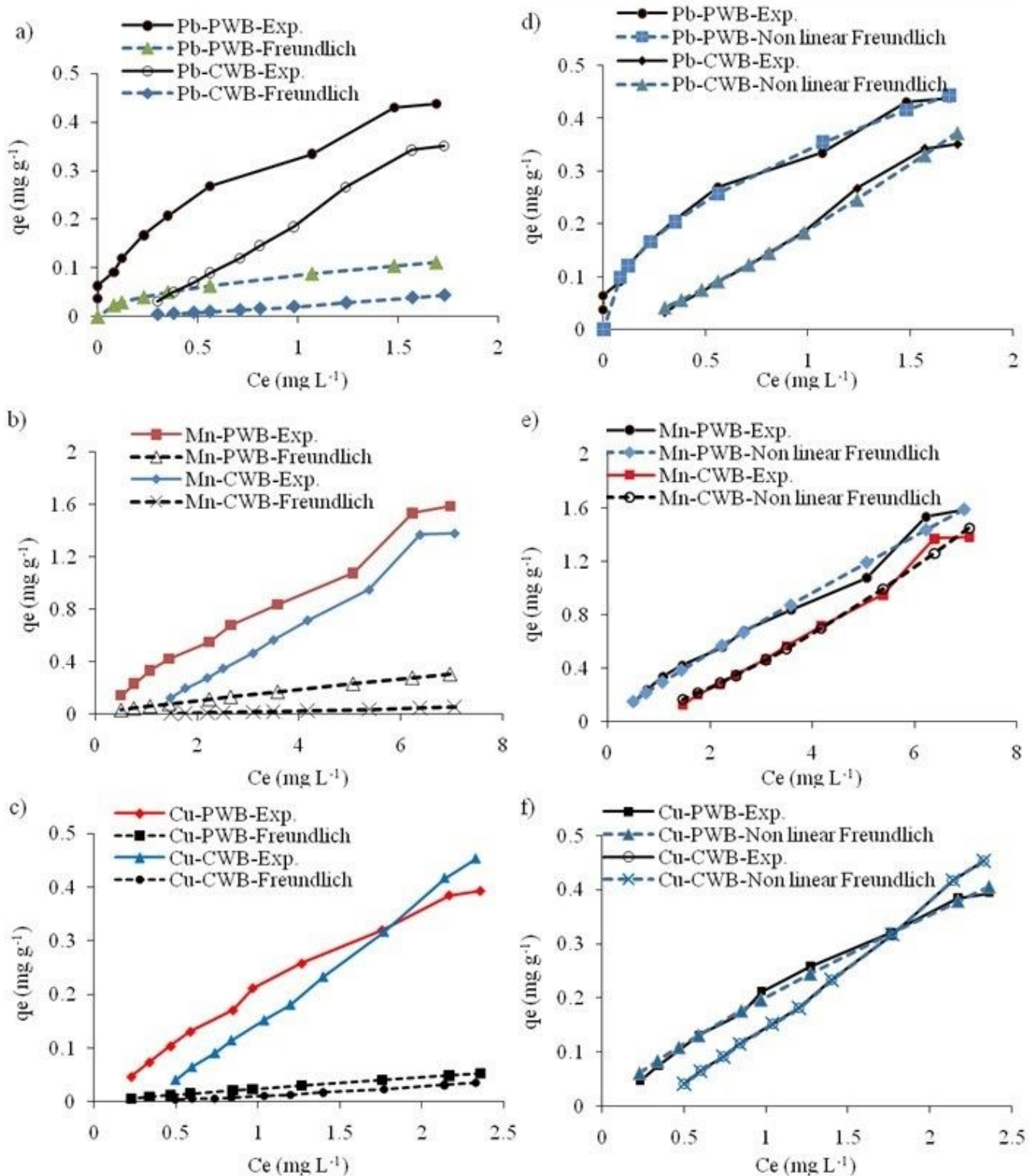


Figure 5

Experimental and predicted adsorption of the heavy metals in leachate onto PWB and CWB using linearized and non-linearized Freundlich equations

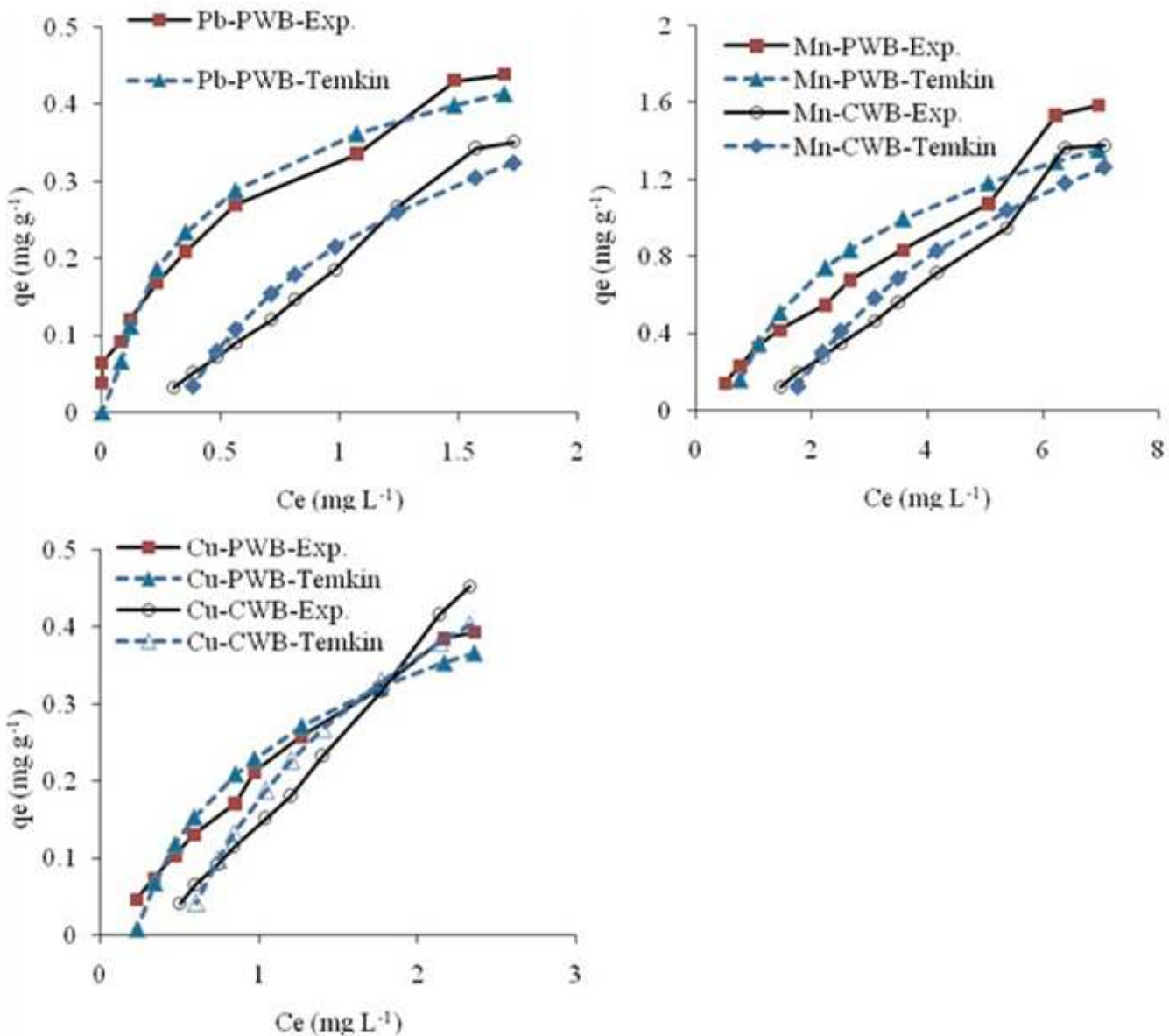


Figure 6

Experimental and predicted adsorption of the heavy metals in landfill leachate onto PWB and CWB using Temkin equation